COMPARATIVE ANALYSIS OF AVALANCHE SEISMIC SIGNALS AND GEODAR DATA AT THE VALLÉE DE LA SIONNE TEST SITE (2018)

P. Roig-Lafon[1]*, C. Pérez-Guillén[1, 2], B. Sovilla[3], E. Suriñach[1, 4], A. Köhler[3], M. Tapia[1, 4] and G. Furdada[1]

[1] *RISKNAT Avalanches Research Group - Institut Geomodels, Universitat de Barcelona (UB), Barcelona 08028, Spain*
[2] *Graduate School of Environmental Studies, Nagoya University, Nagoya, Japan*
[3] *WSL Institute for Snow and Avalanche Research SLF, Davos CH-7260, Switzerland*
[4] *Laboratori d'Estudis Geofísics Eduard Fontserè (LEGEF-IEC), Barcelona 08001, Spain*

ABSTRACT: In this work, we analyze data from three seismic sensors located at strategic locations inside the avalanche path (starting zone, flowing zone and run-out area) and one seismic sensor located in the opposite hillside of the avalanche path, at Vallée de la Sionne test site. Seismic data are correlated in time with GEODAR data. Specifically, the length and the time-frequency features of the seismic data are compared to the flow regimes and front positions recognized from GEODAR data. All observations are complemented with snow cover conditions along the path and before/after photographs. Our results show that seismic data contain relevant information about avalanche flow regimes and thus, can be used to infer characteristics of the avalanche dynamics. Furthermore, the complementarity of the two different measuring systems (seismic and GEODAR) allows us to validate the observations and to enhance the avalanche knowledge from different points of view.

KEYWORDS: Snow avalanches, seismic data, GEODAR, flow regimes, avalanche dynamics

1. INTRODUCTION

Snow avalanches are natural sources of seismic and infrasound waves, which can be recorded and studied for both detection and avalanche dynamics purposes (Suriñach et al., 2001; Biescas et al., 2003; Kogelnig et al., 2011). The knowledge of parameters such as the avalanche size, the run-out distance, the seismic energy dissipation, the front evolution and, its direction and velocity are crucial for avalanche risk mitigation (Vilajosana et al., 2007a; Vilajosana et al., 2007b). In addition, from the analysis of the frequency content of the seismic signals different avalanche flow types can be inferred. Furthermore, the seismic signal duration can be directly linked with the avalanche run-out distance (Pérez-Guillén et al., 2016).

GEODAR (GEOphysical flow dynamics using pulsed Doppler radARradarAR) (Ash et al., 2010; 2014), is a type of radar that is able to penetrate the avalanche powder cloud and monitor the flow of the underlying denser core (Köhler et al., 2016), recognizing different flow regimes and their evolution along the avalanche path. Seven flow regimes and combinations between them where defined using this technique (Köhler et al., 2018).

* *Corresponding author address:*
Pere Roig Lafon. Fac. Ciències de la Terra, Universitat de Barcelona (UB), C/Martí i Franquès s/n. Barcelona 08028, Spain.
tel: +34 934035914
email: p.roig@ub.edu

At present both non-invasive technologies are used as avalanche monitoring systems. Their development and applications are in constant improvement and therefore, the correlation of both type of data can help to improve our understanding of the avalanche behavior as well as to assess the limitations and advantages of both monitoring systems.

2. DATA COLLECTION

The data were recorded at Swiss Vallée de la Sionne avalanche test site (VDLS) which is managed by the WSL Institute for Snow and Avalanche Research SLF (Ammann, 1999; Sovilla et al., 2013). At VDLS avalanches are monitored using multiple time-synchronized instruments. Here we present data corresponding to an avalanche naturally released on 16 February 2018 (avalanche #18-3066).

2.1 Seismic monitoring

The RISKNAT-Avalanche team of the University of Barcelona has four seismic stations installed in VDLS, three inside the avalanche path (starting zone, flowing zone and run-out area respectively) and one seismic sensor located in the opposite hillside of the avalanche path. The sensors are buried into the ground, into caverns (Figure 1).

In the release area (cavern A) a Miniseismonitor passive 3D geophone (2Hz) with a Spider datalogger (Worldsensing) is installed. In the avalanche flowing area (cavern B) there is installed a Mark L-4C-3D passive geophone (1Hz) with a REFTEK-130-01 datalogger (Trimble). In the runout area (cavern C), near the measuring pylon, a Mark L-4C-3D passive geophone (1Hz) and a Lennartz active broadband 3D geophone (20s) are plugged to a REFTEK-130-01 datalogger (Trimble). On the opposite side of the valley

(Bunker), a Mark L-4C-3D passive geophone (1Hz), and a Chaparral 24 infrasound sensor (0,1 Hz) are plugged to the REFTEK-130-01 (Trimble) datalogger (Kogelnig et al., 2011; Pérez-Guillén 2016). All these sensors record continuously during the winter season and are connected to the automatic trigger system of VDLS for recording natural avalanches at high sampling rate. All data are time synchronized. The location of the sensors allows us to record the vibrations produced by the progression of the avalanche flow along the path from different perspectives relative to the avalanche front position.

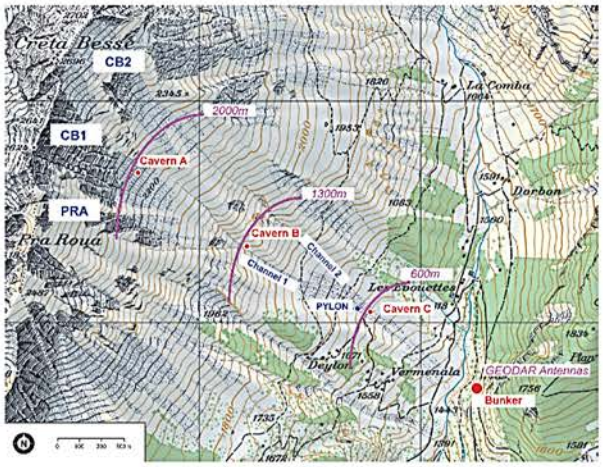

Figure 1 – VDLS experimental site map. Red: seismic stations locations. Blue: Avalanche release areas and track channels (1 and 2). Purple: GEODAR range at cavern positions.

2.2 Seismic interpretation

In order to perform temporal evolution studies of the frequency content, seismic signals sampled at 100/200 Hz and filtered [1 50/100] Hz are represented as spectrograms -a 3D representation (Amplitude, Frequency, time) of the seismograms-. Spectrograms indicate the evolution in time (t) of the frequency (F) content of the signal. Amplitude (A) is represented in colors in logarithmic scale (dB). Spectrograms were calculated using the short-time FFT (Fast Fourier Transform) for time-windows of the signal with a certain overlap. This representation allows us to recognize different sections depending on the location of the seismic sensor relative to the avalanche front (Pérez-Guillén, 2016).

Three main sections can be recognized for the interpretation of the spectrograms (Pérez-Guillén et al., (2016) and references therein):

- **SON** (Signal Onset), when the front of the avalanche approaches the sensor.
- **SOV** (Signal Over), when the avalanche passes over the sensor.
- **SEN** (Signal End), when the avalanche is moving away from the sensor and finally stops.

The **SOV** section can be split in two parts according to the source amplitude: highest amplitudes correspond to the avalanche front and the most energetic part (frontal intermittency region), and lower amplitudes (higher in comparison with SON and SEN sections) correspond to the avalanche tail passing over the sensor (**STA** – Signal Tail).

2.3 GEODAR

GEODAR was developed to obtain high-accuracy data on the dynamic features hidden below the powder cloud (Köhler et al., 2016). Antennas are placed in Bunker, on the opposite side of the Valley, facing the avalanche path (Figure 1). Measurements are performed with an acquisition frequency of 111 Hz and a 0.75 m range resolution (Köhler et al., 2016). GEODAR plots are a color scale representation of logarithmic moving target identification (MTI), allowing to recognize avalanche fronts as the most contrasted parts (Figure 3, bottom). Velocities of the front can be deduced from the plots.

3. JOINT DATA ANALYSIS

On 16 February 2018 at 05:08 UTC a natural avalanche released at VDLS (#18-3066). There is no visual information of the avalanche flowing. The avalanche description was performed with seismic data, GEODAR data and before/after photographs (Figure 2). In Figure 3 the spectrograms of the seismic signals recorded at the 4 caverns and the GEODAR MTI plot are shown, in a common base of time.

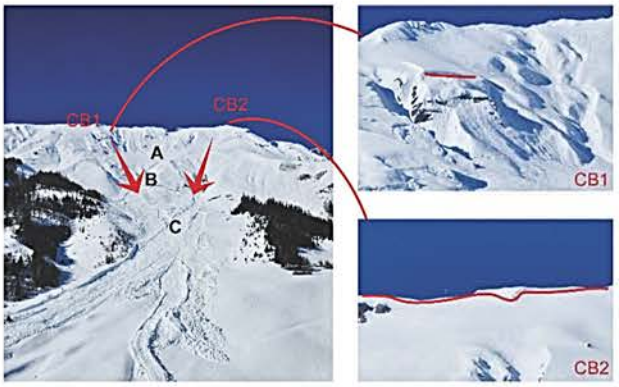

Figure 2 – VDLS photographs after avalanche #18-3066 with release areas (CB1, CB2) and cavern location (A, B, C). Photographs were taken 2 days after the avalanche (Courtesy of Pierre Huguenin).

Both seismic signals and GEODAR data suggest that there were two distinct releases, which produced two main surges. The surges descended along the two channels at different velocities, probably due to the diverse release masses. Photographs suggest two possible release areas at Crêta Besse 1 (CB1) and Crêta Besse 2 (CB2) (Figure 2), both with no evident traces of the trajectory near the release area (only crown scar recognized), fitting with dry and cold flow regimes during the first stages.

The GEODAR data shows the typical characteristics of a transitional flow (Figure 3, Lower panel). The initial part of the avalanche (two fronts) can be recognized from GEODAR as a cold dense regime (CDR). The transition to a warm plug regime (WPR) occurs in the 900 m range when the avalanche front reaches the runout area (Figures 1 and 3) (Köhler et al., 2018). This flow regime transition is reflected in the evolution of the frequency content of the seismic signals, and the relative arrival time of the avalanche front at the different caverns. The trajectory of the two fronts along the path can also be recognized and separated.

All the arrival times of the front to the sensors (SON-SOV) correspond with the front arrivals at the caverns location recognized in the GEODAR MTI plot (Figure 3).

- **Cavern A**: the first avalanche front released from CB1, passed near cavern A at t=-20s (Figure 3 upper panel). The second avalanche front released from CB2 passed over cavern A at t=20s. The difference between the fronts is 40 s. The second front displays higher seismic amplitudes and more complete frequency content. The spectrogram tail (STA) is short (~40s) losing the high frequency content and amplitude considerably fast. These characteristics fit with a cold dense regime (CDR).

- **Cavern B**: the first avalanche front released from CB1 descended along channel 1 and passed over cavern B at t~55-60s (SOV) (range 1300 m in the GEODAR plot) (Figure 3). The second release (CB2) descended along channel 2 and passed the range 1300 m at the same time as the first release (the CB2 front is fastest than the CB1 front). The spectrogram tail is longer than in cavern A (STA), but it loses the frequency content and seismic amplitude abruptly. These characteristics fit with a cold dense regime (CDR) for the first release, and with an Intermittent regime (IR) for the large second release.

- **Cavern C**: The front descending along channel 2 (CB2) passed over the sensor at t~123s. The spectrograms also show full frequency content and high seismic amplitudes. The front coming from channel 1 passed over the sensor 113s later, hitting the pylon at t=236s. The spectrogram tail (STA) is larger and with higher frequency content as in cavern A and B. These characteristics fit with a WPR.

- **Bunker**: The absence of the full frequency content and high seismic amplitudes in the spectrogram indicates that the avalanche did not pass over the sensor. The amplitude and the frequency content progressively increase (below 20Hz) as the avalanche approaches the bottom of the valley. Between cavern C and the bottom of the valley, the flow regime becomes warmer and denser (Figure 2), probably from a WPR to a warm shear regime (WSR). The avalanche front hits the counter slope at t=500s and the spectrogram tail stops suddenly at t=630s. This behavior is also recognizable in GEODAR plot.

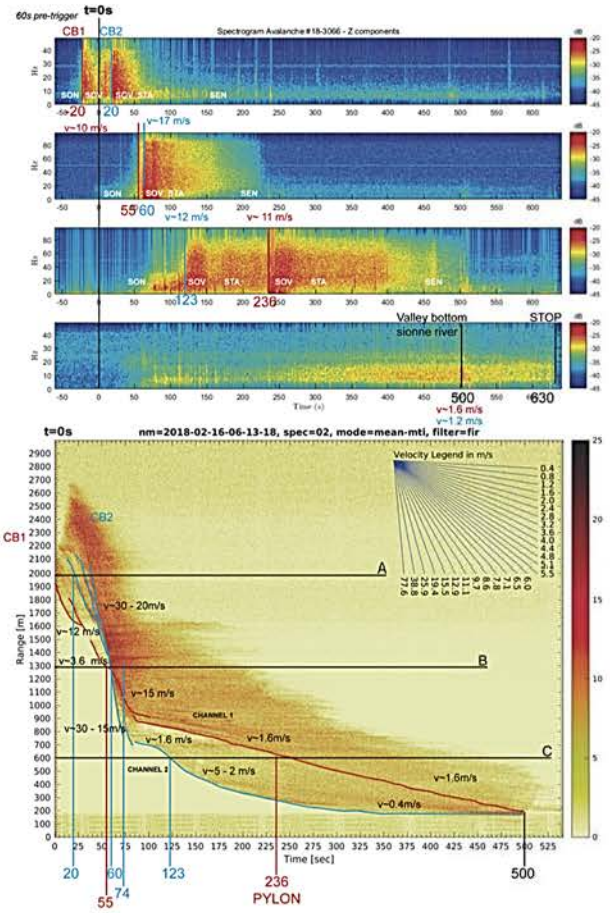

Figure 3 – Avalanche #18-3066. Top: Vertical components of the seismic signal spectrograms recorded at the locations of caverns A, B, C (black lines) and Bunker. Bottom: GEODAR MTI plot. CB1 (red lines) and CB2 (blue lines) indicate the avalanche fronts. Time zero corresponds to the automatic trigger. Seismic signal shows information from 60 seconds before the trigger has been released, from pre-trigger ring buffer data. This pre-trigger allows us to obtain data of the first avalanche front release from CB1 (not observable in GEODAR MTI plot). Significant arrival times and velocities of the fronts are indicated.

The avalanche velocities recognized from the GEODAR MTI plot are higher for the front coming from CB2 (second release) until it reaches the range 700m (between cavern B and C). The avalanche front coming from CB1 (first release) had lower initial velocities. This front also shows a velocity change at range 900m. These changes in velocity in both fronts are related to the flow regime transition from cold to

warm. The average front velocities between the seismic sensors location using the information of the spectrograms fit well with the GEODAT MTI velocity observations (Figure 3).

3.1 Seismic signature polarization

A repetitive signature in seismic signal recorded at cavern C (approx. t=123s), before and after the CB1 SOV was observed. This feature is also recognizable in the signal of cavern D sensor. We deteced high amplitude consecutive peaks in the seismograms that are more evident after filtering the signals between 1-5Hz (Figure 4).

Seismic signal recorded at cavern C presents an increase in amplitudes at t=123s (Figure 3 and 4). The amplitudes decrease after this time. To obtain an insight of the origin of these features we performed a polarization analysis of the different seismic signatures (Vidale, 1986; Jurkevics, 1988; Vilajosana et al., 2008). We interpret these signatures as the signal generated by a moving mass that is approaching the cavern C sensor from channel 1, passes near the sensor to its left side and continues downslope decreasing the amplitude (Figure 4). The bunker seismic signal gives similar information.

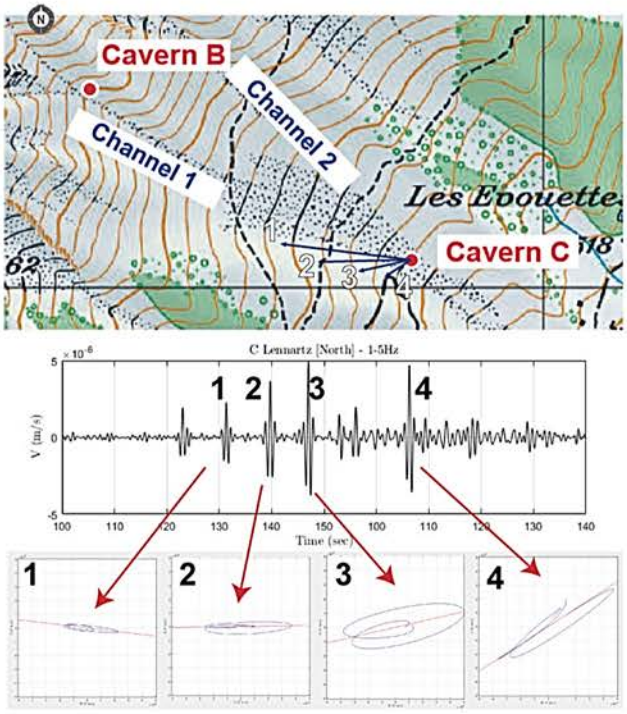

Figure 4 – Upper panel: Extended map of VDLS site with the location of caverns B and C. Middle panel: N-S seismic component of cavern C seismic sensor, filtered between 1-5Hz. The seismic signature is clear, and its polarization analysis shows different azimuth directions, like obtained in rock-fall seismic studies (Lower panel 1, 2, 3 and 4). Represented on a VDLS cartography, the polarization and azimuth directions allow us to reconstruct the path of a punctual mass moving downslope.

As a first approximation, we speculate that the source of these peaks is an independent part of the avalanche passing on the left side of cavern C, when the CB2 avalanche front from channel 2 is reaching cavern C from its right. The repetitive seismic signature infers that the same process is generating it. The increasing amplitude suggests that the source is getting closer to the sensor position. This signature is similar to the signal signature generated by punctual impacts like rockfalls or explosions (Vilajosana et al., 2008). We interpret these ones as an advancing erosion of a warm plug front, overcoming the shear stress resistance repeatedly.

Tour esteems suggest that this plug flow unit forms between caverns B and C, in agreement with the flow regime transition into a warm plug regime (WPR) at 900m range (Figure 3).

4. CONCLUSIONS

Monitoring avalanches using different geophysical instrumentation to acquire different measurements from avalanche flows can be crucial for a better understanding of their behavior. In the absence of previous information on the behavior of avalanches, we can understand how these avalanches have evolved (fronts, directions, velocities) using the combination of seismic data from the 3D seismic sensors placed in the path of the avalanche and the GEODAR MTI diagrams.

Further, a polarization analysis of seismic signatures allows us to track local processes moving downslope, with a clear seismic signature and a specific direction related to the propagation of the flow. These methodologies look promising to allow an automatic characterization of the avalanche flow without using any visual references.

ACKNOWLEDGEMENTS

This research has been possible thanks to the funding of the PROMONTEC PROJECT CGL2017-84720-R (AEI/FEDER, UE) and thanks to AGAUR FI-DGR 2016 (GENCAT) as a funding grant for PhD studies (P.R-L). We are indebted to Pierre Huguenin (SLF, Sion) for the VDLS pictures.

REFERENCES

Ammann, W. J.,1999: A new Swiss test-site for avalanche experiments in the Vallée de la Sionne/Valais. Cold Regions Science and Technology, 30, 3–11.

Ash, M., P. V. Brennan, C. J. Keylock, N. M. Vriend, J. N. McElwaine and B. Sovilla, 2014: Two-dimensional radar imaging of flowing avalanches. Cold Regions Science and Technology, 102, 41–51.

Ash, M, K. Chetty, P. Brennan, J. N. McElwaine and C. Keylock, 2010: FMCW radar imaging of avalanche-like snow movements. IEEE National Radar Conference - Proceedings, 102–107.

Biescas, B., F. Dufour, G. Furdada, G. Khazaradze and E. Suriñach, 2003: Frequency content evolution of snow avalanche seismic signals. Surveys in Geophysics, 24(5–6), 447–464.

Jurkevics, A.,1988: Polarization Analysis of Three-Component Array Data. Bull. Seism. Soc. Am., 78(5), 1725–1743.

Kogelnig, A., E. Suriñach, I. Vilajosana, J. Hübl, B. Sovilla, M. Hiller and F. Dufour, 2011: On the complementariness of infrasound and seismic sensors for monitoring snow avalanches. Nat. Hazards Earth Syst. Sci. 11(8), 2355–2370.

Köhler, A., J. N., McElwaine and B. Sovilla, 2018: GEODAR Data and the Flow Regimes of Snow Avalanches. Journal of Geophysical Research. 123, 23.

Köhler, A., J. N. McElwaine, B. Sovilla, M. Ash, and P. Brennan, 2016: The dynamics of surges in the 3 February 2015 avalanches in Vallée de la Sionne., J. Geophys. Res. Earth Surf. 121, 2192–2210.

Pérez-Guillén, C., M. Tapia, G. Furdada, E. Suriñach, J. N. McElwaine, W. Steinkogler and M. Hiller, 2014: Evaluation of a snow avalanche possibly triggered by a local earthquake at Vallée de la Sionne, Switzerland. Cold Regions Science and Technology, 108, 149–162.

Pérez-Guillén, C., B. Sovilla, E. Suriñach, M. Tapia and A. Köhler, 2016: Deducing avalanche size and flow regimes from seismic measurements. Cold Regions Science and Technology, 121, 25–41.

Pérez-Guillén, C., 2016: Advanced seismic methods applied to the study of snow avalanche dynamics and avalanche formation. PhD Thesis. Universitat de Barcelona.

Sovilla, B., J. N. McElwaine, W. Steinkogler, M. Hiller and F. Dufour, 2013 : The full-scale avalanche dynamics test site Vallée de la Sionne. In International Snow Science Workshop (pp. 3–10).

Suriñach, E., G. Furdada, F. Sabot, B. Biescas and J. M. Vilaplana, 2001: On the characterization of seismic signals generated by snow avalanches for monitoring purposes. Annals of Glaciology, 32, 268–274.

Vidale, J. E., 1986: Complex polarization analysis of particle motion. Bull. Seism. Soc. Am., 76(5), 1393–1405.

Vilajosana, I., G. Khazaradze, E. Suriñach, E. Lied, and K. Kristensen, 2007a: Snow avalanche speed determination using seismic methods. Cold Regions Science and Technology, 49, 2–10.

Vilajosana, I., E. Suriñach, G. Khazaradze, and P. Gauer, 2007b: Snow avalanche energy estimation from seismic signal analysis. Cold Regions Science and Technology, 50, 72–85.

Vilajosana, I., E. Suriñach; A. Abellán; G. Khazaradze, D. García, and J. Llosa, 2008: Rockfall induced seismic signals: case study in Montserrat, Catalonia. Nat. Hazards Earth Syst. Sci. 8(4), 805–812.